Journal of Innovative Technology, Vol. 3, No. 2, pp. 27-37, September 2021
http://doi.org/10.29424/JIT.202109_3(2).0004


# Real-Time Power Split Strategy of Hybrid Energy Storage System for Electric Vehicle

Li-Shuo You [1] and Chang-Hua Lin [2*]

## ABSTRACT

High charge/discharge current is a major factor that shortens the health of the lithium battery. For this reason, once the electric vehicle accelerates or decelerates, the required amount of power fluctuates greatly. Therefore, this paper suggests using a supercapacitor as another energy storage component. This device is thought to be suitable for high charge/discharge current because it is based on the use of the battery semi-active hybrid energy storage architecture. Vehicle load can be generally split by the proposed real-time power split strategy. For this reason, the battery can provide a smoother power curve, and the supercapacitor bears precipitous load required for acceleration and deceleration to better prevent the lithium battery from producing a steep change in current. Finally, hybrid energy storage system (HESS) platform is built and tested. Also, HESS circuit and power split strategy are modeled in Simulink, and the results derived from the simulated and tested waveforms are validated experimentally by operating the proposed real-time power split strategy..

*Keywords:* hybrid energy storage system, power split strategy, electric vehicle.

## 1. INTRODUCTION

Transportation vehicles are being electrified, and this trend will continue to surge in 2021. However, most common electric vehicles nowadays use a single energy storage element, such as lithium batteries. Notably, if the lithium batteries of electric vehicles are driven under different road conditions and so suffer precipitous load, the battery life will be greatly degraded and aging. As suggested by Karden *et al*. 2007, the battery life will be reduced by 200 to 300 cycles when the Ni-MH battery repeatedly undergoes the changing of load, and so the better operating range of batteries is to discharge to the 20 ~ 50% interval of the battery's rated capacity. Secondly, with regard to the characteristics of lithium iron phosphate batteries, based on the results obtained from the experiments carried out by Omar *et al*. 2014, to operate this at high ambient temperatures, high discharging current or too low state of charge are all the main reasons for the accelerated aging batteries to occur. With this in mind, if the battery only uses a single energy storage element to cope with the load of electric vehicles, it will lead to over-design of battery module specifications, and so increase the size and weight of the system (Shen *et al*. 2014).

In order to better solve the aforesaid problems, many research papers have proposed a hybrid energy storage system (HESS) to do so. The ultimate goal of this system is twofold: (1) to combine high-power density supercapacitors to provide or absorb steep changing load transient and (2) to allow the supply of the smooth and stable average load by a battery with high energy density to occur. Also, the different electrical characteristics of the two storage components complement each other's advantages and disadvantages, so as to further reduce the possibility of using batteries under the frequent changing of load, thereby extending the battery life.

The state of the art of HESS architecture divided into four types is depicted in Fig. 1. Firstly, as for the Passive HESS (Zheng *et al*. 2001; Peng *et al*. 2004; Omar *et al*. 2010), both the battery and the supercapacitor are directly connected in parallel, so the energy cannot be controlled and distributed. In addition, the supercapacitor only works at the first moment of discharge, for the terminal voltage of the supercapacitor is clamped by the battery voltage, and so it loses the expected effect of adding supercapcitor. Secondly, regarding the semi-active battery HESS (Wang *et al*. 2017; Kuperman *et al*. 2013; Wang *et al*. 2017; Dusmez *et al*. 2015), the battery uses a bidirectional converter connected to the DC bus, the advantage of this architecture is that the battery discharged/charged current can be controlled by converter, and the supercapacitor acts as an energy buffer to absorb and release steep changing loads. Furthermore, since the purpose of the battery is to provide average power energy, and the converter maximum power does not need to be designed to reach the full load power of the electric vehicle, it just can be designed with average power. Next, concerning the semi-active supercapacitor HESS (Song *et al*. 2015; He *et al*. 2013; Zhang *et al*. 2020), since the energy of the supercapacitor is not limited by the DC bus voltage, the energy of the supercapacitor can be properly used. However, the supercapacitor must provide the frequently changing load. In this case, to better design the bidirectional converter, the almost full load power of the electric vehicle should be achieved, and so the converter needs to have a wide voltage range adjustment and good transient response to achieve stable bidirectional power transmission. Finally, as to the fully active HESS (Eren *et al*. 2009; Yoo *et al*. 2008),

Manuscript received July 13, 2021; revised July 28, 2021; accepted August 2, 2021.

[1] Master Student, National Taiwan University of Science and Technology, Taipei City, Taiwan 106335, R.O.C.

[2*] Professor (corresponding author), National Taiwan University of Science and Technology, Taipei City, Taiwan 106335, R.O.C. (e-mail: link@mail.ntust.edu.tw)

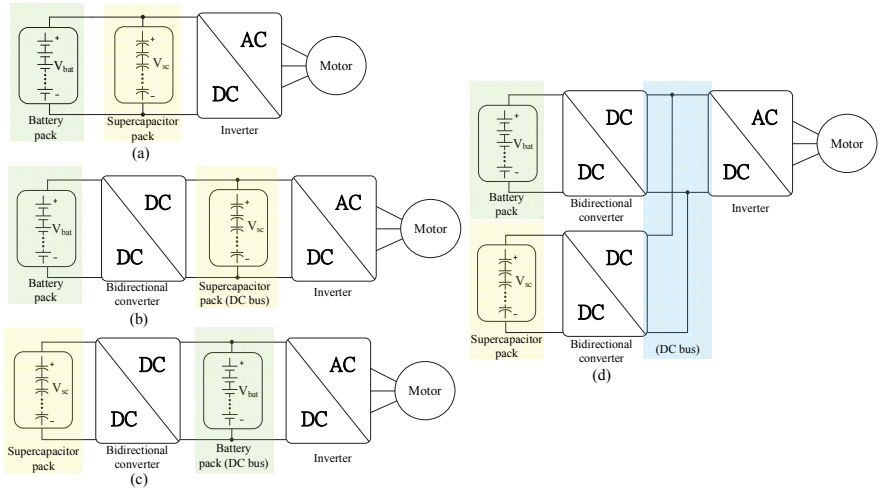


**Fig. 1 Simplified circuit schematic of HESS topologies (a) passive HESS (b) battery-semi HESS (c) supercapacitor-semi HESS (d) full active HESS.**

battery and supercapacitor are connected to the bidirectional converter. The DC bus voltage can be adjusted by two bidirectional converters, so the DC bus voltage is the most stable, but its system complexity and cost are also higher than the above three architectures.

This paper demonstrates the architecture of battery semi-active hybrid energy storage system. In this system, the bidirectional converter uses the synchronous rectification interleaved converter, and the digital signal controller (DSP) is considered to implement the real-time power split strategy and so to control the power converter through the use of the electric vehicle load curve specification design battery pack, supercapacitor pack and power converter.

## 2. REAL-TIME POWER SPLIT STRATEGY

At the beginning, as shown in Fig. 2, the speed curve of electric vehicle running in the city was used as the simulation for the actual experiment. This speed curve specification was obtained from the U.S. environmental protection agency. This is generally adopted to test the condition of light vehicles driving in the city. We use the model known as "Explore the Electric Vehicle Reference Application" released by MATLAB. This model composed of electric motors, batteries, transmissions and powertrains, as illustrated in Fig. 3, is generally used to complete the electric vehicle model and set the required UDDS speed curve so as further to obtain the power curve that battery needs to bear in the UDDS driving cycle of the electric vehicle. This is clearly shown in Fig. 4, where the x-axis is time and y-axis is power. In order to match the specifications of the equipment in the laboratory and verify the power distribution strategy, the maximum peak value of the UDDS load curve is scaled down to 2.51 kW, thus keeping the original load curve discharging and recharging energy change trends. As depicted in Fig. 4, the load change of the curve before t = 500s is the most severe, so in subsequent simulation and experiment, the load curve is set for t = 0 ~ 500s for analysis.

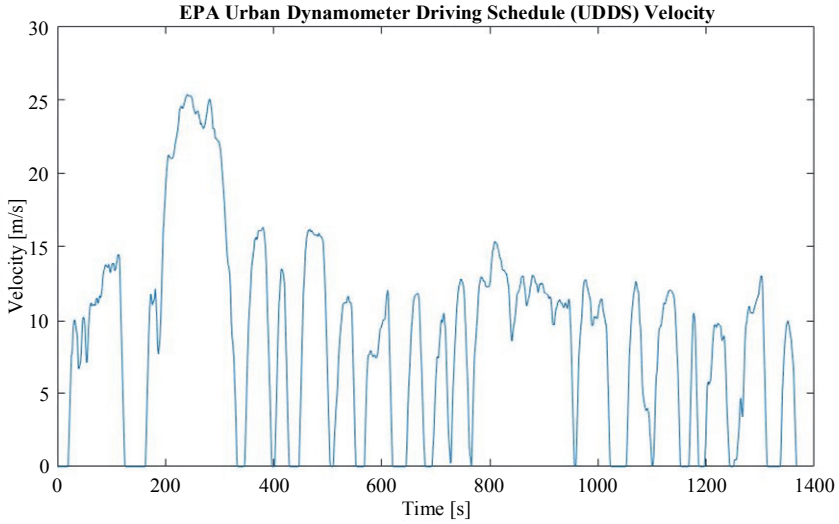


**Fig. 2 Urban Dynamometer Driving Schedule (UDDS) standard.**

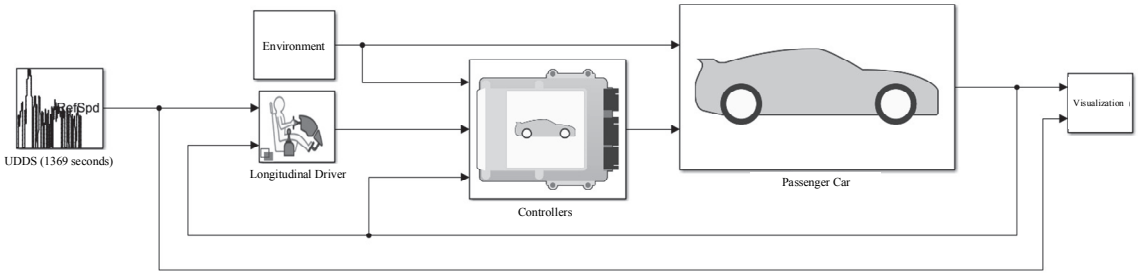


**Fig. 3 Electric model built in Simulink**

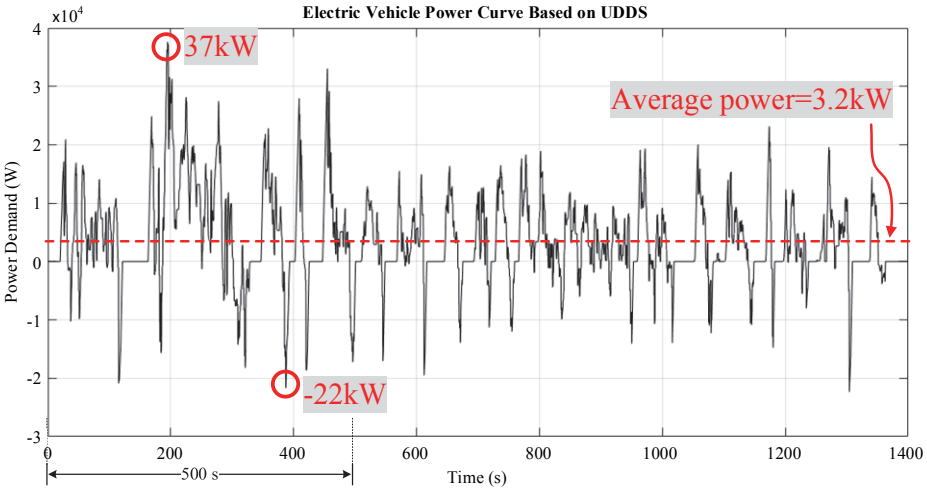


**Fig. 4 Electric vehicle's power curve running with UDDS driving cycle**

Before power distribution, it is necessary to obtain the power variation of the electric vehicle in real time. Since the supercapacitor of the battery semi-active HESS is located on the DC bus, according to the characteristics of the voltage change of the supercapacitor, it is used with a digital controller to sample periodically, as presented in Fig. 5.

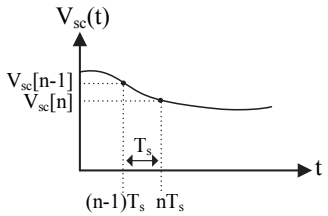


**Fig. 5 Sketch of real-time power evaluation by supercapacitor**

The energy $\Delta W_{sc}$ released or absorbed by the supercapacitor during the unit sampling period can be obtained, as shown in Eq. (1), where $V_{sc}[n]$ is the current sampling voltage value of the supercapacitor, and $V_{sc}[n-1]$ is the previous sampled voltage value of the supercapacitor. When $\Delta W_{sc}$ is positive, this means that supercapacitor is discharging; on the contrary, it is recharged energy when the vehicle's braking system is applied.

$$\Delta W_{sc}[n]=\frac{C_{sc}}{2}(V_{sc}^2[n-1]-V_{sc}^2[n]) \tag{1}$$

The instantaneous power of the supercapacitor ($P_{sc}$) can be obtained by dividing the energy by the unit sampling period ($T_s$), as shown in Eq. (2), since the load change of the electric vehicle is in seconds, unit sampling period design with 0.02s is enough to estimate the power variation of electric vehicle.

$$P_{sc}[n]=\frac{\Delta W_{sc}[n]}{T_s}=\frac{C_{sc}}{2T_s}(V_{sc}^2[n-1]-V_{sc}^2[n]) \tag{2}$$

The load power ($P_{load}$) is the sum of the instantaneous power of the supercapacitor and the previous output power of the converter ($P_{conv}[n-1]$), as shown in Eq. (3). With this method, through the physical characteristics of supercapacitor, the load of the electric vehicle can be obtained in real time, and no additional output current sensor is needed.

$$P_{load}[n]=P_{sc}[n]+P_{conv}[n-1] \tag{3}$$

After obtaining the real-time load change, since the battery output power is controlled by the power converter, in order to correlate the power provided by the battery with the vehicle load change, the real-time power estimated power ($P_{load}$) is input into the digital filter u[n], and output y[n] can smooth the load of electric vehicles with drastic changes, as shown in Fig. 6. Then, the smoothed power amount is used as the reference power amount based on the rule-based control.

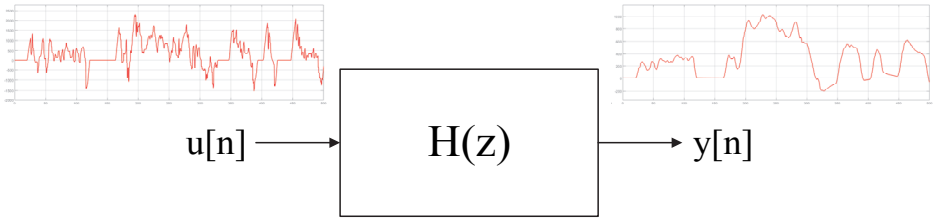


**Fig. 6 Sketch of power curve smoothing**

The design of the digital filter H(z) can refer to the analog first-order RC low-pass filter (LPF), and its frequency domain expression is as Eq. (4), where τ is the RC time constant.

$$H(s)=\frac{1}{s\tau+1} \tag{4}$$

According to Euler backward approximation s = (z-1)/($T_s$·z), where $T_s$ is the same sampling period as that of real-time power estimation. Eq. (4) can be converted to z by Euler backward approximation to obtain Eq. (5).

$$H(z)=\frac{T_s \cdot z}{(z-1)\tau+T_s \cdot z} \tag{5}$$

Eq. (5) through the inverse z-transformation, the digital filter expression of the discrete signal can be obtained as Eq. (6).

$$y[n]=\frac{\tau}{\tau+T_s} \cdot y[n-1]+\frac{T_s}{\tau+T_s} \cdot u[n] \tag{6}$$

where

y[n]: the current output value of LPF

y[n-1]: the previous output value of LPF

u[n]: the current input value of LPF

Eq. (6) can be realized through a digital controller used to smooth the calculated load power and serve as the key basis for the energy ratio between the battery and the supercapacitor.

Although the smooth load curve has been allocated to the battery by load smoothing method, and the battery output current is limited by controlling the power converter to enable the battery to withstand drastic load changes, the DC bus is determined by the supercapacitor terminal voltage. However, this is especially true when the load changes precipitously because the bus terminal voltage will still fluctuate. In order to control the DC bus terminal voltage to maintain within the inverter's operating voltage range 65 ~ 85V, this control method is added.

According to the voltage value of the supercapacitor, the system plans five regular control modes, as shown in Fig. 7. The purpose of this is to not only make the energy distribution of the battery and the supercapacitor more flexible but also make the DC bus voltage and the system more stable. The structural details of Each of the modes are clearly illustrated, and they are as follows:

Energy compensation mode (65V < $V_{sc}$ ≤ 73V): Since the DC bus voltage is about to be lower than the lower limit of the set voltage range (65V), energy compensation is performed through Eq. (7), where $P_{bat}^{max}$ is the maximum output power of the battery. When

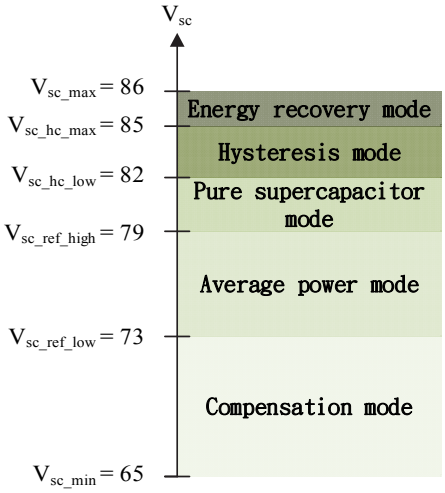


**Fig. 7 Sketch of rule-based control**

the $V_{sc}[n]$ is lower, the output power of the converter is higher, and the DC bus voltage is compensated to the intermediate value (75V) as soon as possible to avoid the voltage falling below the lower limit of the inverter's working voltage. The power flow of the circuit is shown in Fig. 8.

$$P_{conv}=(P_{bat}^{max}-P_{avg}) \cdot \frac{73-V_{sc}[n]}{73-65}+P_{avg} \tag{7}$$

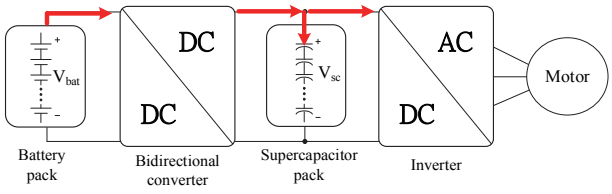


**Fig. 8 HESS power flow of compensation mode**

Average power mode (73V < $V_{sc}$ ≤ 79V): Since the voltage of the supercapacitor is in the middle of the predetermined DC bus voltage range, the system is relatively stable at this time, so the battery can output the smoothed load command through the converter. The supercapacitor is responsible for absorbing or providing additional load transient changes. In this mode, the output power command quantity of the converter is $P_{conv}$ = $P_{avg}$[n]. The power flow of the circuit is shown in Fig. 9.

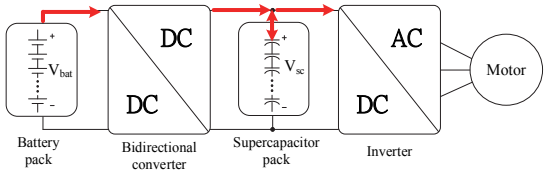


**Fig. 9 HESS power flow of average power mode**

Supercapacitor mode (79V < $V_{sc}$ ≤ 82V): Since the DC bus voltage is sufficient at this time, in this mode, the converter is turned off, and the supercapacitor will handle all the required discharging and recharging energy of the electric vehicle load. At this time $P_{conv}$ = 0W. The power flow of the circuit is illustrated in Fig. 10.

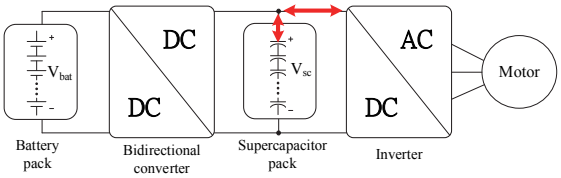


**Fig. 10 HESS power flow of pure supercapacitor mode**

Hysteresis control mode (82V < $V_{sc}$ ≤ 85V): In this mode, the DC bus voltage is close to the upper limit voltage value (86V). In order to avoid only one judgment formula, which causes the converter to shut down and start frequently, this mode is added. When the electric vehicle is braking, load energy is recharging supercapacitor, the converter will start aftter $V_{sc}$ reach the hysteresis upper limit voltage (85V), and recycle the excess energy to the battery. However, when the energy recovery mode is activated, $V_{sc}$ needs to reach the lower limit of hysteresis voltage (82V), the converter will shut down again and return to pure supercapacitor mode, as shown in Fig. 11.

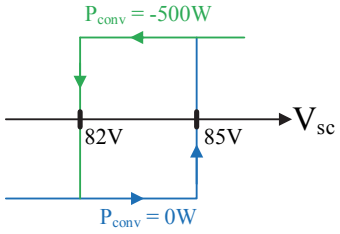


**Fig. 11 Sketch of hysteresis mode**

Energy recovery mode ($V_{sc}$ > 85V): In this mode, it is close to the upper limit voltage of the converter, so the excess energy is recharged to the battery to ensure that the DC bus voltage does not exceed the upper limit (86V), at this time $P_{conv}$ = –500W, approximately 1C charging current to charge battery. The power flow of the circuit is shown in Fig. 12.

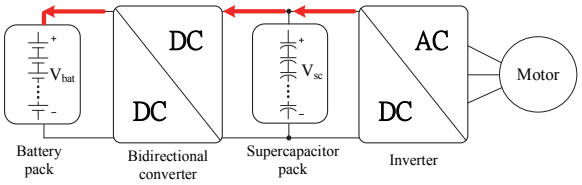


**Fig. 12 HESS power flow of energy recovery mode**

## 3. HESS DESIGN CONSIDERATIONS

The hardware of the HESS includes a lithium battery pack, a supercapacitor pack, and a power converter. The design process considerations are given as follows:

### 3.1 The determination of the load power variation range of the electric vehicle

The maximum power of the electric motor assumed is 3 kW in this paper, of which the load variation range is –1448 W ~ 2511 W, the most severe load variation interval is t = 187 ~ 205s, as shown in Fig. 13, and the inverter input voltage range is 65 V ~ 85 V. By referring to above-mentioned conditions, the design of battery semi-active hybrid energy storage system is performed.

The larger the lithium battery capacity is, the longer the endurance is. However, the endurance parameters that may help endurance were not considered in this research paper. That is because the lithium battery is connected to the input terminal of the boost converter, and so the consideration is given to the duty cycle (D) of the boost converter. For example, when the input voltage is the maximum value, and the output voltage is the minimum value of 65 V, there will be a minimum value of D. Suppose the minimum value of D is designed to be 0.1, according to the boost converter voltage gain, the maximum input voltage is 58.5 V, which means that the maximum operating voltage of the design lithium battery pack should not exceed 58.5 V.

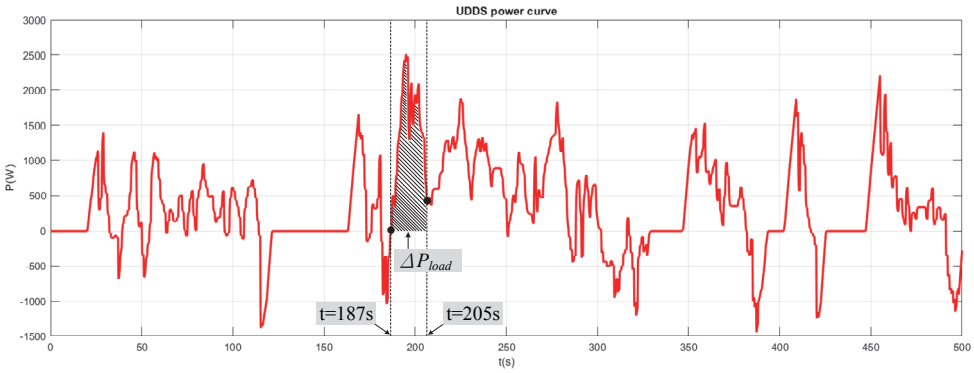


**Fig. 13 Simulation and experiment electric vehicle load curve**

### 3.2 Limit to the capacity of the lithium battery pack and working voltage considerations

In terms of battery pack specifications, $LiFePO_4$ batteries are used. Although the energy density is lower than lithium ion batteries, their inherent advantages include better safety, longer life and lower costs. The specifications of the single battery used in the actual measurement are shown in Table 1. The battery pack involves 16 series and 1 parallel, the voltage working range is 48 ~ 57.6 V, the working voltage flat range is 52.8V, the rated capacity is 18AH, and the discharge rate was usually 2C ~ 5C. In order to avoid the excessive discharge current, the maximum battery discharge current is assumed to be 30A (the manufacturer recommends less than 2C, take 1.67C), this helps multiply the flat zone working voltage 52.8V and so get $P_{bat}^{\max}$ to be 1600W.

**Table 1 Single $LiFePO_4$ battery specification**

| Parameter | Value | Unit |
|---|---|---|
| maximum voltage | 3.6 | V |
| nominal voltage | 3.3 | V |
| cut-off voltage | 3.0 | V |
| C-rate | 18 | AH |

### 3.3 The importance of the supercapacitor pack capacity and working voltage considerations

Since the supercapacitor pack is directly connected to the DC bus, the voltage value specification of the supercapacitor pack is the same as the input voltage range of the inverter, and the capacitance value of the supercapacitor pack will be determined by the UDDS power curve where the load changes most precipitously, as shown in Fig. 13. The maximum load change interval is from t = 187 ~ 205 s.

Therefore, after integrating the energy in the interval of t = 187~205 s, the total energy required for the acceleration of the electric vehicle during this period is $E_{load}$ = 35189 J. This load energy is shared by the supercapacitor and the converter. Assuming that the supercapacitor voltage starts from the middle value of the DC bus voltage ($V_{sc\_ref}$ = 75 V), the supercapacitor voltage needs to be greater than the lower limit voltage ($V_{sc\_min}$ = 65 V). Meanwhile, assuming that the converter outputs at a constant power of 1300 W in this interval, therefore, from t = 187 ~ 205 s, the converter can provide a total of $E_{conv}$ = 23400 J, and the supercapacitor is responsible for providing $E_{sc} > E_{load} - E_{conv}$ = 11789J. According to Eq. (8), it can be obtained that the capacitance needs at least 15.7 F.

$$E_{sc} = \frac{C_{sc}}{2}(V_{sc\_ref}^2 - V_{sc\_min}^2) \tag{8}$$

In order to both meet the upper limit of the inverter's working voltage(85V) and ensure the withstand voltage of a single supercapacitor in a safe range, a single supercapacitor with a capacitance of 500F was selected to do so together with 30 series and 1 parallel. So the rated capacity of the supercapacitor pack is 16.6 F, and the rated voltage is 90 V. The specifications of a single supercapacitor are shown in Table 2.

**Table 2 Single supercapacitor specification**

| Parameter | Value | Unit |
|---|---|---|
| rated voltage | 3.0 | V |
| capacitance | 500 | F |
| equivalent series resistor | 4.5 | mΩ |
| maximum discharge current | 230 | A |

### 3.4 The selection of the converter input\output voltage range and maximum power considerations

The converter input and output voltage range is exactly the same as the lithium battery pack voltage variation range and the inverter input voltage range. The design consideration of the maximum power value of the converter is actually the average power value in the most drastic range of load changes, when t = 187 ~ 205 seconds, the average power is 1560 W, as shown in Fig. 13. In order to enable the supercapacitor voltage to be quickly compensated under heavy load, the maximum power value was designed to increase by 25%, so 2000 W was taken as the maximum power value of the converter.

The bidirectional power converter uses a two-phase synchronous rectification converter, as depicted in Fig. 14. The input and output terminals are connected to battery pack and supercapacitor pack, respectively. The power flow from the battery to the supercapacitor is built in the boost mode, and the supercapacitor to the battery is built in buck mode. The converter specifications are provided in Table 3.

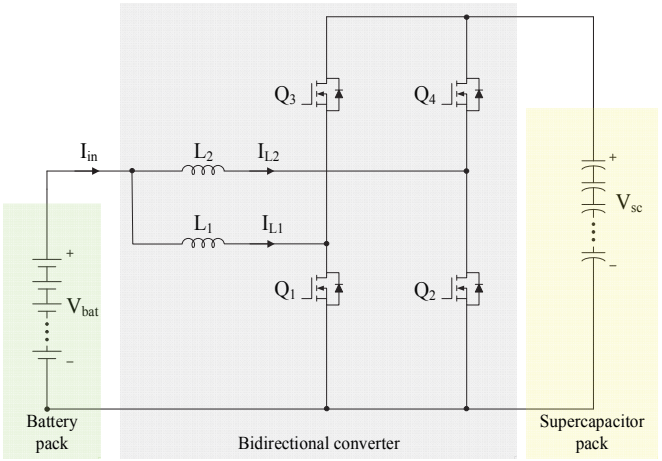


**Fig. 14 Two Phase synchronize buck/boost converter**

**Table 3 Two phase synchronize converter specification**

| Parameter | Value | Unit |
|---|---|---|
| input voltage range | 48 ~ 57.6 | V |
| output voltage range | 65 ~ 85 | V |
| switching frequency | 100 | kHz |
| maximum power | 2000 | W |
| inductance | 50 | μH |

When designing the inductance, when the input voltage is usually 53V in the flat area of the battery and the output voltage is 85V, the maximum duty cycle is calculated as follows

$$D=\frac{V_o-V_i}{V_o}\cong 0.376 \tag{9}$$

Assuming that the converter efficiency is 0.95 and the maximum output power is 2000 W, the input current can be derived as follows

$$I_{in}=\frac{P_o}{V_i\eta}\cong 39.72\ \text{A} \tag{10}$$

The single-phase inductor current $I_{L1}$, $I_{L2}$ is half of the input current $I_{in}$, and the single-phase inductor current ripple is designed to be 20% of the DC value, so the inductance can be obtained as follows

$$L=\frac{V_i}{\Delta i_L}DT_s\cong 50\ \mu\text{H} \tag{11}$$

## 4. SIMULATION MODELLING AND EXPERIMENT RESULT VERIFICATION

Fig. 15 shows the required equipment and schematic diagram of HESS. Fig. 16 shows the HESS actual experiment platform. In the following experiment and simulation, the HESS provides a power range from −1448 W to 2511 W, a load and supercapacitor voltage range of 65 V to 85 V, and a battery voltage range of 48 V to 57.8 V. Among them, the flat battery voltage is 52.8 V, and the voltage range of the interleaved converter is exactly the same as that of the battery and supercapacitor, and so it can operate at ±2000 W. The preset conditions before the formal test are that the supercapacitor voltage $V_{sc}$ is pre-charged to the middle value of the inverter input voltage range 75V, and $V_{bat}$ is pre-charged to the flat working voltage 53V. The UDDS load curve uses the dynamic power curve, as shown in Fig. 13, for the following simulation and actual test verification.

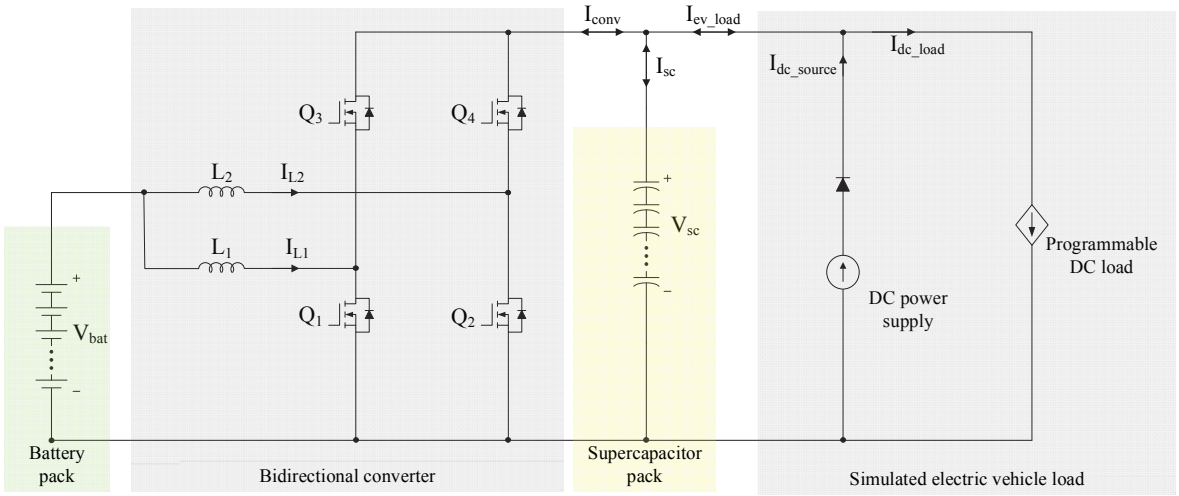


**Fig. 15 Schematic of HESS experiment platform**

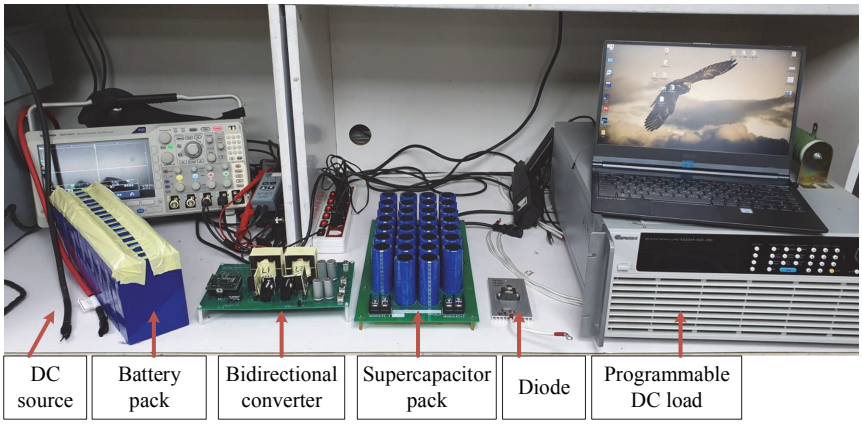


**Fig. 16 HESS experiment platform**

Fig. 17 illustrates how to form a simulated electric vehicle load waveform through a DC programmable load and a DC power supply. First of all, although the programmable load machine cannot control the amount of power curve, it can only control the amount of dynamic current curve, and so the load curve in Fig. 13 is divided by the intermediate value of the inverter's input voltage range of 75V and converted into a load current curve, which maintains a similar electric vehicle load curve. To base this on Kirchhoff's current law, $I_{ev\_load} = I_{dc\_load} - I_{dc\_source}$, so after shift of the load current curve is caused by the negative maximum current, the data are burned into the programmable load machine, and the DC power supply provides the maximum negative current. In this case, it can implement the dynamic load characteristics of electric vehicle.

Fig. 18 shows the modeling of a hybrid energy storage system. The hardware modeling includes batteries, power converters, supercapacitors, and the UDDS load curve. The power converter was modeled by an average model; software modeling including real-time power estimation, power smoothing method, rule-based control and PI negative feedback control were used to verify the feasibility of the proposed power split strategy through the system modeling for the comparison of the results derived from the subsequent actual experiments.

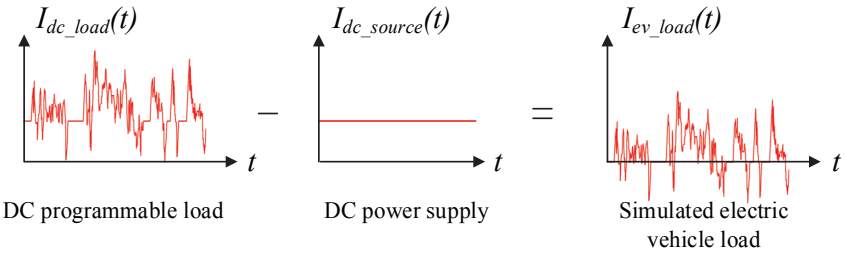


**Fig. 17 Explain how to implement simulated electric vehicle load curve**

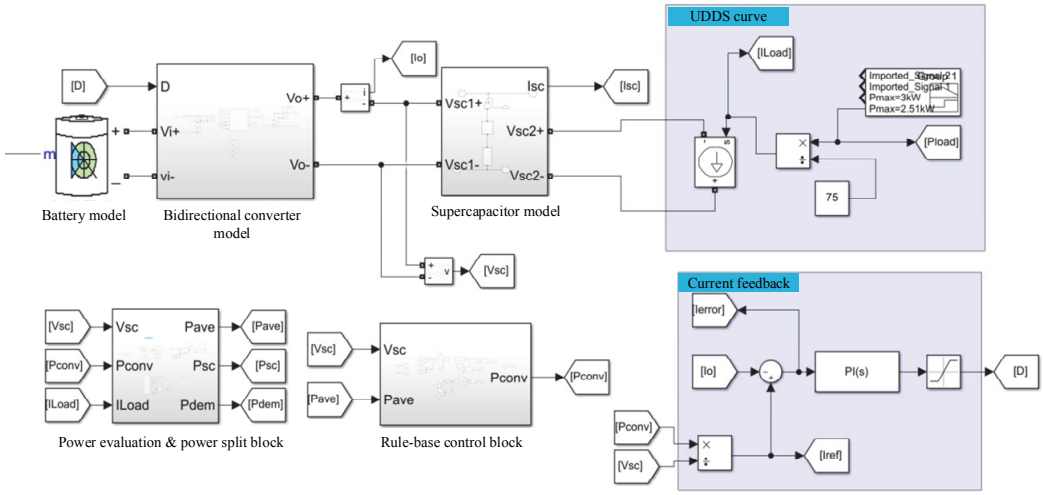


**Fig. 18 HESS simulation model built in Simulink.**

Fig. 19 shows the simulation results of HESS operated under UDDS load conditions. The waveforms from top to bottom are supercapacitor voltage ($V_{sc}$), supercapacitor current ($I_{sc}$), electric vehicle load current ($I_{ev\_load}$) and converter output current ($I_{conv}$). $I_{ev\_load}$ curve in the figure is obtained by dividing the UDDS power curve, as shown in Fig. 13, by the intermediate value of the DC bus voltage of 75 V. As can be seen from Fig. 19, $V_{sc}$ curve can tell, based on the rule-based control, that the supercapacitor voltage range can be stably operated within the specified range of 65V ~ 85V. Furthermore, HESS with a power split strategy can distribute the electric vehicle load current between the supercapacitor and the lithium battery. The supercapacitor current ($I_{sc}$) can withstand the precipitous changing load of the electric vehicle, and the battery current ($I_{conv}$) curve mainly depends on the converter to output a smooth load. Therefore, the battery current trend will be the same as that of the converter's output current, and this can greatly reduce both the battery current stress and the repeated charging and discharging current.

In addition, as shown in Fig. 19, two solid red lines are used to mark the voltage value of the supercapacitor, $V_{sc\_ref\_low}$ = 73 V and $V_{sc\_ref\_high}$ = 79 V. Both values are used to verify the mode conversion of the rule-based control strategy, which can be referred to Fig. 7. First, when the time is from t = 192 ~ 248 s, the supercapacitor voltage is lower than the lower limit voltage value of in the average mode (73V), so the rule-based control strategy enters the energy compensation mode. Power command of converter is followed by Eq. (7), it can be observed from the figure

that when the $V_{sc}$ goes lower, the output current of the converter will increase rapidly, and $V_{sc}$ will be returned to the intermediate value of the DC bus voltage 75V as soon as possible; Second, when the time is from t = 248 ~ 309 s, the $V_{sc}$ is in the range of 73V to 79V, so rule-based control strategy enters the average power mode. Meanwhile, the converter power command is followed by the power passing through the digital low-pass filter. It can be seen from the figure that the output current of the converter is relatively smooth. Finally, when the time is from t = 309 ~ 353 s, $V_{sc}$ exceeds 79 V, so rule-based control strategy enters the pure supercapacitor mode. In this mode, the converter is turned off, all load changes are suffered by the supercapacitor. Regarding this load condition, $V_{sc}$ does not exceed the upper limit voltage of 85 V, and so the energy recovery mode is not entered under the entire road condition.

Fig. 20 shows the experimental results of HESS operated under the UDDS load specifications, where CH1 is the converter output current ($I_{conv}$), CH2 is the supercapacitor current ($I_{sc}$), CH3 is the electric vehicle load current ($I_{ev\_load}$), and CH4 is supercapacitor voltage ($V_{sc}$). Among them, CH4 has adjust DC level offset, so that the oscilloscope presents a subtle change in the voltage of the supercapacitor. Observably, $V_{sc}$ under the whole road condition is 66.7V ~ 83.9V. It can be therefore verified that the DC bus terminal voltage is stably controlled within the set range, based on the rule-based control strategy. Since the upper limit voltage of 85V is not exceeded, the whole road condition is not operating in the energy recovery mode.

As can seen from Fig. 20, $I_{conv}$ outputs a relatively smooth current curve, while the precipitous changing load current curve is suffered by $I_{sc}$. This confirms the effectiveness of HESS with the power split strategy, and so HESS can effectively reduce the regeneration energy of electric vehicles to recharge the lithium battery. And the lithium battery only needs to provide a smooth and relatively stable current waveform.

Among them, when $I_{ev\_load}$ reaches a full load value of 32.2A, $I_{sc}$ takes 16.5A, and $I_{conv}$ allocates 15.7A. Compared with a single energy storage system, the current stress of the lithium battery is reduced by 51.24% at full load.

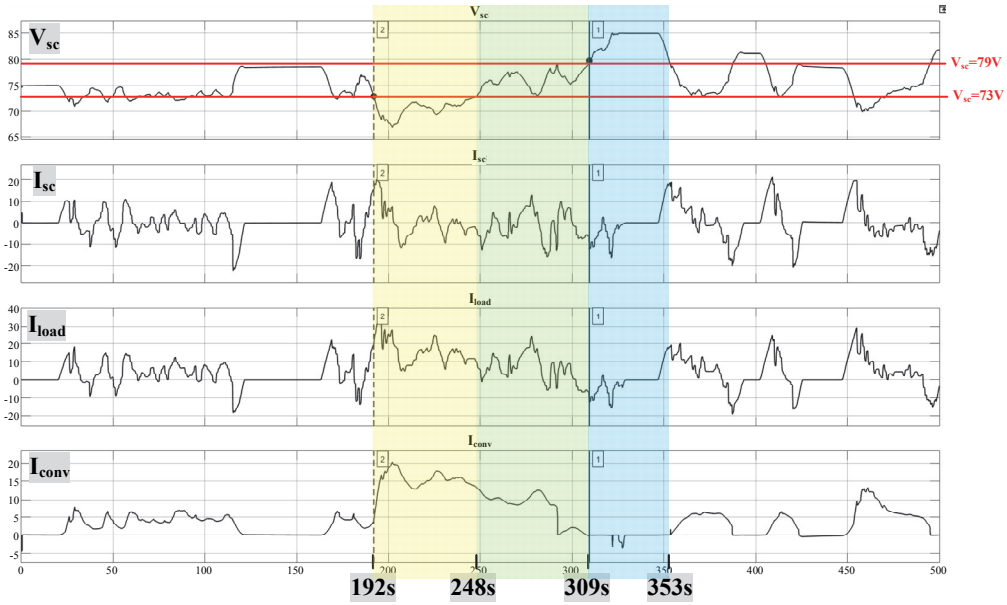


**Fig. 19 HESS with UDDS driving cycle simulation results**

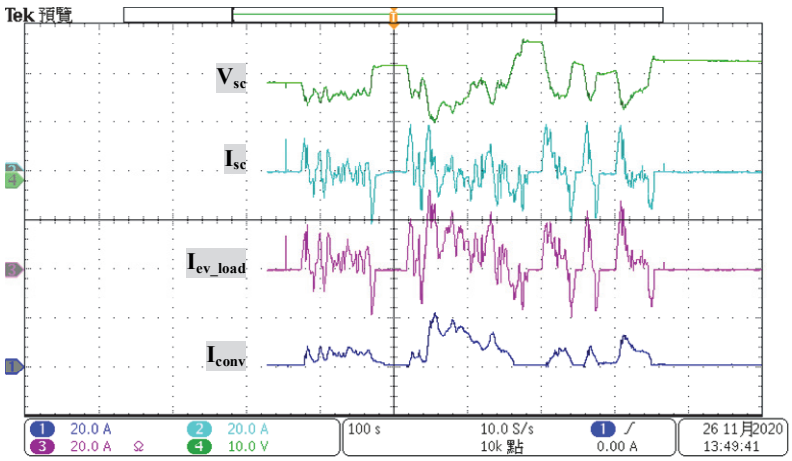


**Fig. 20 HESS with UDDS driving cycle experiment results**

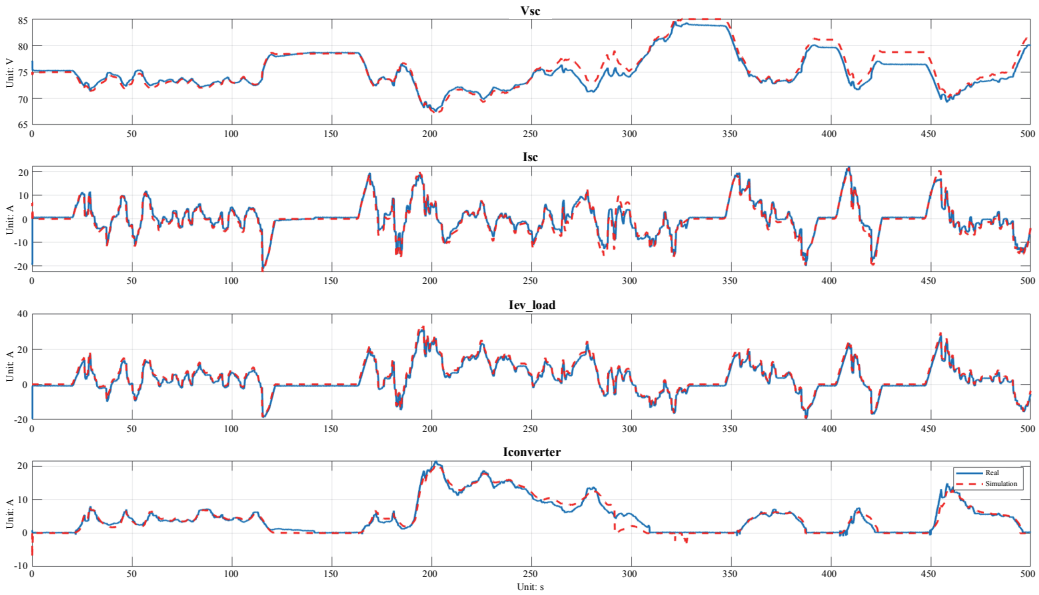


**Fig. 21 Simulation and experiment results comparison**

Figure 21 is illustrated by reading the data provided in Figs. 20 and 19 in the same graph for comparison. Among them, the solid blue line refers to the actual measured waveform, and the red dashed line represents the simulated waveform. The converter output current trends of the two curves are the same. This can verify the accuracy of the hardware modelling of the hybrid energy storage system, and so the power distribution strategy can be realized by a digital controller.

In this paper, the ESR of the supercapacitor is not considered. Since the ESR value of the supercapacitor is actually very low, it will only slightly affect the sampling value of $V_{sc}$, temperature rise, and system efficiency. However, it will not affect the stability of the power distribution strategy, for the variation of $V_{sc}$ is employed to calculate the real-time power evaluation of $P_{sc}$.

It is noted that the energy recovery mode is not included in both the simulation and the actual measurement results. This is mainly because when the proposed system is operated g in the UDDS road conditions, the recovered energy cannot lead the supercapacitor voltage to exceed the upper limit voltage in the hysteresis control ($V_{sc\_hc\_max}$ = 85 V). Therefore, neither the actual measurement nor the simulation result will enter the energy recovery mode. Meanwhile, if the upper limit voltage value of the proposed hysteresis control is directly changed or other driving conditions that recover more energy (for example, a long downhill road) are considered , then the RB control can enter the energy recovery mode.

## 5. CONCLUSIONS

The battery semi-active hybrid energy storage system with the proposed real-time power split strategy has been proposed in this paper. To be specific, a real-time power split strategy can be implemented by a digital controller to better control the power converter. The load energy of the electric vehicle is appropriately distributed to the battery and the supercapacitor, so that the supercapacitor could withstand precipitous current curve when the acceleration and deceleration phases takes place, and so the battery would provide a smoother load curve according to the power split strategy. This real-time power estimation is based on the physical characteristics of the supercapacitor, combined with the periodic sampling by a digital controller through which the load change of the electric vehicle in real time without adding a current sensor in output line can be calculated. The core concept of power distribution is to pass the vehicle load through a digital filter, so that the power provided by the battery is related to the instant load change, and the DC bus voltage is relatively stable, based on the rule-based control, and so this makes HESS more flexible when it comes to energy provision. Finally, this research paper employed Simulink simulation modeling and the actual experiment platform of HESS. The results indicate that HESS with power split strategy can greatly reduce battery current by allocating part energy to supercapacitor. At the peak load, the battery pack provides 48.8% load current, and the supercapcitor pack withstands 51.2% load current, which extends the battery life.

## REFERENCES

Dusmez, S., Hasanzadeh, A., and Khaligh (2015). "A. Comparative analysis of bidirectional three-level DC-DC converter for automotive applications." *IEEE Trans. Ind. Electron*, **62**, 3305-3315.

Eren, T., Erdinc, O., Gorgun, H., Uzunoglu, M., and Vural, B (2009). "A fuzzy logic based supervisory controller for an FC/UC hybrid vehicular power system." *Journ. Hydro. Energy*, **34**, 8681-8694.

He, H., Xiong, R., Zhao, K., and Liu, Z. (2013). "Energy management strategy research on a hybrid power system by hardware-in-loop experiments." *Applied Energy*, **112**, 1311-1317.

Karden, E., Ploumen, S., Fricke, B., Miller, T., and Snyder, K. (2007). "Energy storage devices for future hybrid electric vehicles." *Journ. Power Sources*, **168**, 2-11.

Kuperman, A., Aharon, I., Malki, S., and Kara, A. (2013). "Design of a semiactive battery-ultracapacitor hybrid energy source." *IEEE Trans. Power Electron*, **28**, 806-815.

Omar, N., Monem, M.A., Firouz, Y., Salminen, J., Smekens, J., Hegazy, O., and Van Mierlo, J. (2014). "Lithium iron phosphate based battery–Assessment of the aging parameters and development of cycle life model." *Applied Energy*, **113**, 1575-1585.

Omar, N., Mierlo, J.V., Verbrugge, B., and Bossche, P.V.D. (2010). "Power and life enhancement of battery-electrical double layer capacitor for hybrid electric and charge-depleting plug-in vehicle applications." *Electrochi. Acta*, **55**, 7524-7531.

Peng, F.Z., Li, H., Su, G.J., and Lawler, J.S. (2004). "A new ZVS bidirectional DC-DC converter for fuel cell and battery application." *IEEE Trans. Power Electron*, **19**, 54-65.

Shen, J., Dusmez, S., and Khaligh, A. (2014). "Optimization of sizing and battery cycle life in battery/ultracapacitor hybrid energy storage systems for electric vehicle applications." *IEEE Trans. Ind. inform*, **10**, 2112-2121.

Song, Z., Hofmann, H., Li, J., Han, X., and Ouyang, M. (2015). "Optimization for a hybrid energy storage system in electric vehicles using dynamic programing approach." *Applied Energy*, **139**, 151-162.

Tran, D.D., Vafaeipour, M., El Baghdadi, M., Barrero, R., Van Mierlo, J., and Hegazy, O. (2020). "Thorough state-of-the-art analysis of electric and hybrid vehicle powertrains: Topologies and integrated energy management strategies." *Renewable and Sustainable Energy Reviews*, **119**, 109596.

Wang, B., Xu, J., Wai, R.J., and Cao, B. (2017). "Adaptive sliding-mode with hysteresis control strategy for simple multimode hybrid energy storage system in electric vehicles." *IEEE Trans. Ind. Electron*, **64**, 1404-1414.

Wang, B., Xu, J., Xu, D., and Yan, Z. (2017). "Implementation of an estimator-based adaptive sliding mode control strategy for a boost converter based battery/supercapacitor hybrid energy storage system in electric vehicles." *Energy Convers. and Manage*, **151**, 562-572.

Yoo, H., Sul, S.K., Park, Y. and Jeong, J. (2008). "System integration and power-flow management for a series hybrid electric vehicle using supercapacitors and batteries." *IEEE Trans. Ind. Applic*, 44, 108-114.

Zhang, Q. and Li, G. (2020). "Experimental study on a semi-active battery-supercapacitor hybrid energy storage system for electric vehicle application." *IEEE Power Electron*, **35**, 1014-1021.

Zheng, J.P., Jow, T.R., and Ding, M.S. (2001). Hybrid power sources for pulsed current applications. *IEEE Trans. Aero. and Elect. Systems*, **37**, 288-292.